Groundwater for Sustainable Development 26 (2024) 101262

Contents lists available at ScienceDirect

Groundwater for Sustainable Development

journal homepage: www.elsevier.com/locate/gsd

Research paper

Integration of geospatial-based algorithms for groundwater potential characterization in Keiskamma Catchment of South Africa

Kgabo Humphrey Thamaga [a,*], Sinesipho Gom [a], Gbenga Olamide Adesola [b], Naledzani Ndou [a], Nndanduleni Muavhi [c], Mthunzi Mndela [d], Phila Sibandze [a], Hazem Ghassan Abdo [e], Thabang Maphanga [f], Gbenga Abayomi Afuye [g,h], Benett Siyabonga Madonsela [f], Hussein Almohamad [i]

[a] *Department of GIS and Remote Sensing, University of Fort Hare, Alice, South Africa*
[b] *Department of Geology, University of Fort Hare, Alice, South Africa*
[c] *Department of Environmental Sciences, University of South Africa, Pretoria, South Africa*
[d] *Department of Livestock and Pasture, University of Fort Hare, Alice, South Africa*
[e] *Geography Department, Faculty of Arts and Humanities, Tartous University, Tartous, Syria*
[f] *Department of Environmental and Occupational Studies, Cape Peninsula University of Technology, Corner of Hanover and Tennant Street, Zonnebloem, Cape Town, South Africa*
[g] *Department of Geography and Environment Science, University of Fort Hare, Alice, South Africa*
[h] *Geospatial Application, Climate Change, and Environmental Sustainability Lab–GACCES, University of Fort Hare, Alice, Eastern Cape Province, South Africa*
[i] *Department of Geography, College of Arabic Languages and Human Social Sciences, Qassim University, Buraydah, 51452, Saudi Arabia*

HIGHLIGHTS

- The study characterizes GWPZ using AHP and FR in drought-prone environments.
- The estimated performance of the models in characterizing GWPZs revealed that FR performed better than AHP.
- GWPZ are beneficial for decision-making.

GRAPHICAL ABSTRACT

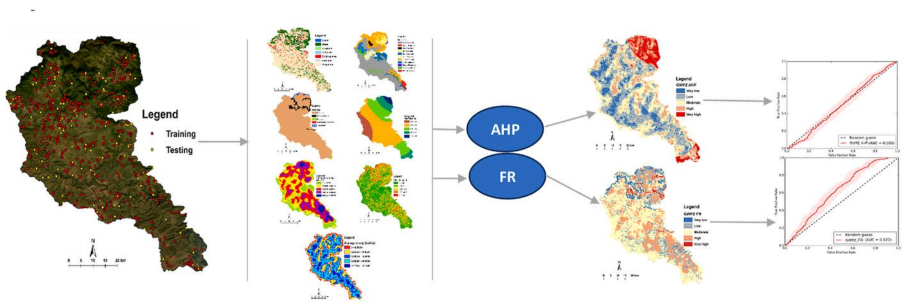

ARTICLE INFO

Keywords:
Area under curve
Climate change
Groundwater management
Hydrogeology
Rainfall variability
Water scarcity

ABSTRACT

Groundwater supports over 2.4 billion people across the globe and is critical to food security. The spatial dynamics of groundwater vary from place to place. The irregularity of groundwater resource exploitation is recognized in drought-prone areas, putting pressure on the resource. Hence, accurate groundwater potential characterization is critical for sustainable development and management of groundwater, particularly in drought-prone environments. Therefore, this study aimed at utilizing remote sensing satellite data and geospatial-based (analytical hierarchy process (AHP) and frequency ratio (FR)) algorithms to characterize groundwater potential zones (GWPZs) in the Keiskamma Catchment of South Africa. Seven (7) selected factors, including geology, soil type, slope, rainfall, drainage density, lineament density, and land use land cover, were

* Corresponding author.
E-mail address: KThamaga@ufh.ac.za (K.H. Thamaga).

https://doi.org/10.1016/j.gsd.2024.101262
Received 2 November 2023; Received in revised form 24 June 2024; Accepted 25 June 2024
Available online 29 June 2024

assigned weights based on the AHP and FR algorithms. The validation results showed that the FR model performed better than the AHP, with the area under curve (AUC) accuracies of 62% and 50%, respectively. Based on the findings of this study, we infer that FR is more reliable than AHP when characterizing GWPZ. Lastly, GWPZ maps produced will be beneficial for improving efficient planning, management strategies, and decision-making.

1. Introduction

Groundwater is the main potable water supply for over 2.4 billion people and is crucial to global food security (United Nations, 2015). In drought-prone regions, groundwater utilization is critical for maintaining rural farmers' livelihoods and ensuring food security (Yadav et al., 2023). It supplies 40% of the water used by the agricultural sector and one-third of the industrial water demand (Boretti and Rosa, 2019). Groundwater distribution is uneven due to the spatiotemporal variation in rainfall, regional differences in geomorphology, and diversity of geologic media. Despite these variations, Dar et al. (2021) highlighted that the global rate of groundwater abstraction is as high as 27%, 42%, and 36% for the agricultural, industrial, and domestic sectors, respectively. Groundwater demands are incessantly increasing due to rapid population growth, expansion of irrigated farming areas, and industrialization (Das et al., 2017). Fulfilling these rising water demands is crucial, especially in arid and semi-arid regions, even though this imposes a significant strain on groundwater. Excessive groundwater withdrawal to sustain the population and agricultural production causes irreversible soil subsidence, resulting in deterioration in groundwater recharge, water table depth, and the drying up of wells in several areas (Rafiei et al., 2022).

The issue of water scarcity is aggravated by erratic rainfall as a consequence of climate change and variability, making groundwater resources more vulnerable (Busico et al., 2019). Inadequate surface water associated with rising temperatures results in the rapid drying up of aquifers, leading to water scarcity in drought-prone regions (Urama and Ozor, 2010). However, developing sufficient water supply systems is still a major concern in South Africa, a semi-arid nation with limited water resources (Edokpayi et al., 2018). The rural communities are the most vulnerable and impacted group in South Africa, accounting for 13 million people without adequate sanitation and six million people without access to safe drinking water (Basson, 2012). Some of the poorest and most rural communities in South Africa are situated in the Eastern Cape Province (Moyo et al., 2022). The rural communities in the Keiskamma water catchment depend on groundwater as the primary water source, and securing access to groundwater is a major concern (Grecksch, 2015). Therefore, delineating groundwater potential zones (GWPZ) in the study area is crucial to developing sustainable groundwater use plans and management strategies.

Over the years, a variety of modeling approaches have been devised to assess the spatial characterization of groundwater potential zones (GWPZs), and these approaches relied on field surveys, geophysical models, and hydrogeological drilling for testing (Virupaksha and Lokesh, 2021; Echogdali et al., 2022; Adesola et al., 2023a,b; Ait Haddou et al., 2023). These approaches are appropriate for identifying hydrological features, but they are expensive, lack spatial representation, are arduous, and time-consuming (Muavhi et al., 2022). To counter these challenges, geospatial approaches emerged as an effective instrument for modeling GWPZ by integrating geological formation, topographical forms, climatic conditions, the pattern and intensity of land use land cover, and soil characteristics (Zhao et al., 2022). Geospatial approaches provide detailed information at wider spatial scales, save time, and are cost-effective (Tweed et al., 2007). Researchers have tested these approaches using models to predict groundwater yield and identify the optimal model for deciphering GWPZ mapping for effective water resource management (Muavhi et al., 2022).

To characterize GWPZs based on the parameters, relationships, and contributions to groundwater movements and accumulations, a variety of statistical, expert assessment, and deterministic approaches were investigated (Muavhi et al., 2022; Das and Pal, 2019; Marjuanto et al., 2019; Karimi-Rizvandi et al., 2021; Abdo et al., 2024; Adesola, 2024). Various researchers used multiple-criteria decision-making (MCDM) approaches such as Data Envelopment Analysis (DEA) (Halder et al., 2022; Opricovic and Tzeng, 2002; Tzeng and Huang, 2011; Hwang and Yoon, 1981). Researchers have recognized the AHP as an efficient decision-making technique to characterize GWPZs (Oikonomidis et al., 2015; Doke et al., 2021; Adesola et al., 2023a,b; Ikirri et al., 2023). Oikonomidis et al. (2015) used an integrated GIS/RS method based on AHP to identify potential groundwater areas in Tirnavos, Greece. The findings provided significant information and maps that local authorities could use for groundwater exploitation and management. Doke et al. (2021) integrated GIS-based MCDM, AHP, and remote sensing to map recharge potential zones in India's hard rock basaltic terrain. It was concluded that the techniques applied in the study showed great efficiency and precision and, therefore, may be used to evaluate the groundwater potential zone in similar drought-prone regions worldwide. Ikirri et al. (2023) used GIS and AHP models to assess potential groundwater areas in the Ifni basin, situated in the western Anti-Atlas range of Morocco. The area under curve (AUC = 80%) showed the good predictive accuracy of the AHP method.

The AHP consists of breaking complicated problems into an order of criteria and evaluating the relative importance of each criterion with pairwise comparison (Doke et al., 2021). Another useful tool is the frequency ratio (FR), which is known as a bivariate numerical approach that estimates spatial relationships relating to the independent variables (boreholes) and the dependent variables (groundwater controlling factors) to assign ranking estimates to each category (Das and Pardeshi, 2018). In many diverse situations, these geospatial-based algorithms use several criteria, including – climate, topography, and land use data, to assess groundwater vulnerability and predict groundwater occurrences in larger areas. Studies have demonstrated that the FR model is more effective and reliable than the knowledge guided AHP algorithm. For instance, (Muavhi et al., 2022) compared AHP and FR techniques to delineate GWPZs. The outcomes of this study revealed that the FR model outperformed AHP, with AUCs of 72% and 60%, respectively. El Ayady et al. (2023) employed mathematical modeling (FR), and geomatics tools (remote sensing and GIS) to map and assess potential groundwater zones in the Anzi sub-basin, western Anti-Atlas, Morocco. The FR model's validity was confirmed through the ROC (receiver operating characteristic) curve analysis, showing a reliability value of 82.5% for the FR model in mapping groundwater potential. These models need to be explored in drought-prone areas where water security is the main challenge.

Therefore, in this study, we integrated geospatial-based algorithms and remote sensing tools to define the importance of various factors such as land use, land cover, soil type, slope, and geology to delineate GWPZ. The study objectives are to (i) determine the factors that significantly influence GWPZ, (ii) evaluate modeling algorithms for characterizing GWPZs, and (iii) assess the model performance using receiver operating characteristic (ROC) curves and borehole variation maps of the Keiskamma Catchment. This was achieved by assigning appropriate weights to the identified thematic layers of groundwater controlling factors and employing the overlaying analysis technique. The delineated GWPZ was authenticated using borehole data and the ROC method. The aptitude for geospatial-based algorithms is critical in understanding the status of groundwater, enhancing decision-making, policy implementation, and the endorsement of artificial recharge structures in drought-prone areas. The opportunity of the performing algorithm can further be applied on a larger spatial area and contribute towards achieving sustainable development goals.

2. Materials and methods

2.1. Description of the study area

The study was conducted in the Keiskamma Catchment area of the Eastern Cape, South Africa (Fig. 1). The area lies within latitude: 33°17′S and longitude: 27°29′E geographical coordinates. The catchment covers an area of 2443 km^2. The Tyume, Gxulu, and Chalumna rivers are the main drainages in the catchment. These rivers rise in the Amatole mountains and flow 263 km before discharging into the Indian Ocean at the Hamburg estuary. The area has a 20–30% rainfall deficit and is prone to drought. The catchment's mean annual rainfall varies from 43 mm to 95 mm. The mean annual temperature ranges between 11 °C and 38 °C in winter and summer, respectively. Keiskamma Catchment is also situated at an elevation ranging from 2 to 1937 m above sea level. The soil characteristics of the catchment give the spatially dominant soil types in the catchment expressed as World Reference Base for Soil Resources (WRBSR) names, as provided in the field of the SOTERSAF_-Dominant Soils layer resulting from the underlying sandstone, shale, and red mudstone geological units.

Geologically, the Keiskamma Catchment is dominated by the rocks of the Adelaide and Tarkastad Subgroups belonging to the Beaufort Group of the Karoo Supergroup, with widespread dolerite intrusions (Johnson et al., 1997). The catchment is primarily made up of sedimentary rocks like mudstones, shales, and sandstones, which have been extensively intruded by the Karoo dolerites in the form of dykes and sills (van Breda Weaver, 1991). According to Verdoodt et al. (2003), the catchments' coastal boundary comprises semi-consolidated sand, high coastal dunes, and unconsolidated beach sand covering older sedimentary rocks. Furthermore, extremely erodible soils originating from mudstones and shales are common across the catchment (Verdoodt et al., 2003). Dondo et al. (2010) noted that the fractured and jointed aquifers in the southern Karoo basin indicate semi-confined conditions. However, well-developed aquifer regions are found in the fractured zones caused by dolerite intrusions where high-yielding boreholes have been documented (Woodford and Chevallier, 2002). DWAF (2008) reported that most groundwater boreholes in the study area show very low yields with constant flow rates of less than 2 L/s.

2.2. Data acquisition and preparation of inventory maps

To achieve the main objective of this study, the geo-environmental datasets were acquired (Table 1) for delineating and mapping GWPZ in the Keiskamma Catchment. The datasets were pre-processed to extract the groundwater controlling factors: slope, geology, rainfall, drainage density, soil, lineaments, and land use land cover. Photo-lineaments were mapped from Landsat 8 OLI data (image ID: LC08_L1TP_170082_20220709_20220719_02_T1) using principal component image from PCA and for automatic lineament extraction using LINE algorithm of PCI Geomatica software. The confirmed

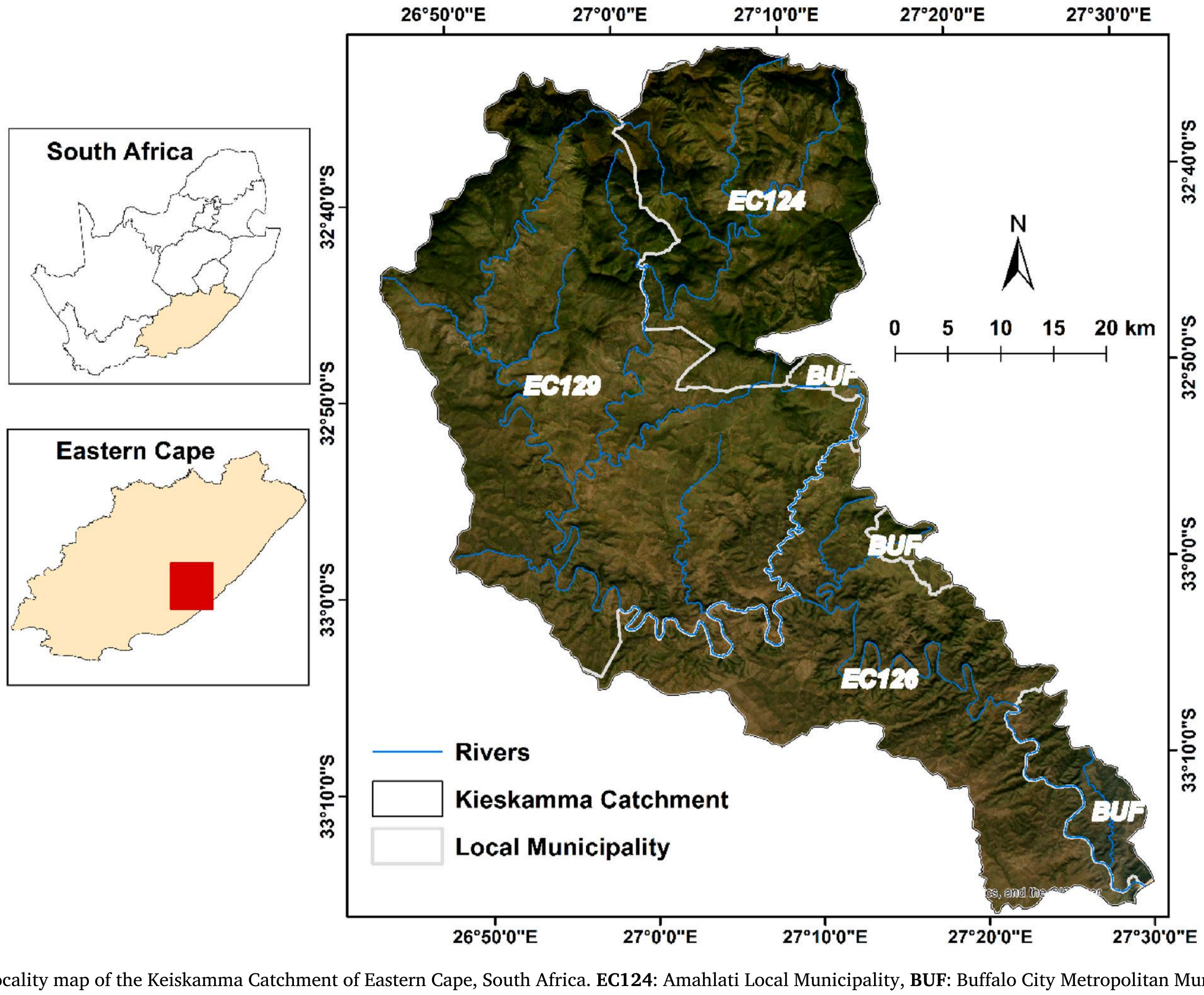

Fig. 1. Locality map of the Keiskamma Catchment of Eastern Cape, South Africa. **EC124**: Amahlati Local Municipality, **BUF**: Buffalo City Metropolitan Municipality, **EC126**: Ngqushwa Local Municipality, and **EC129**: Raymond Mhlaba Local Municipality.

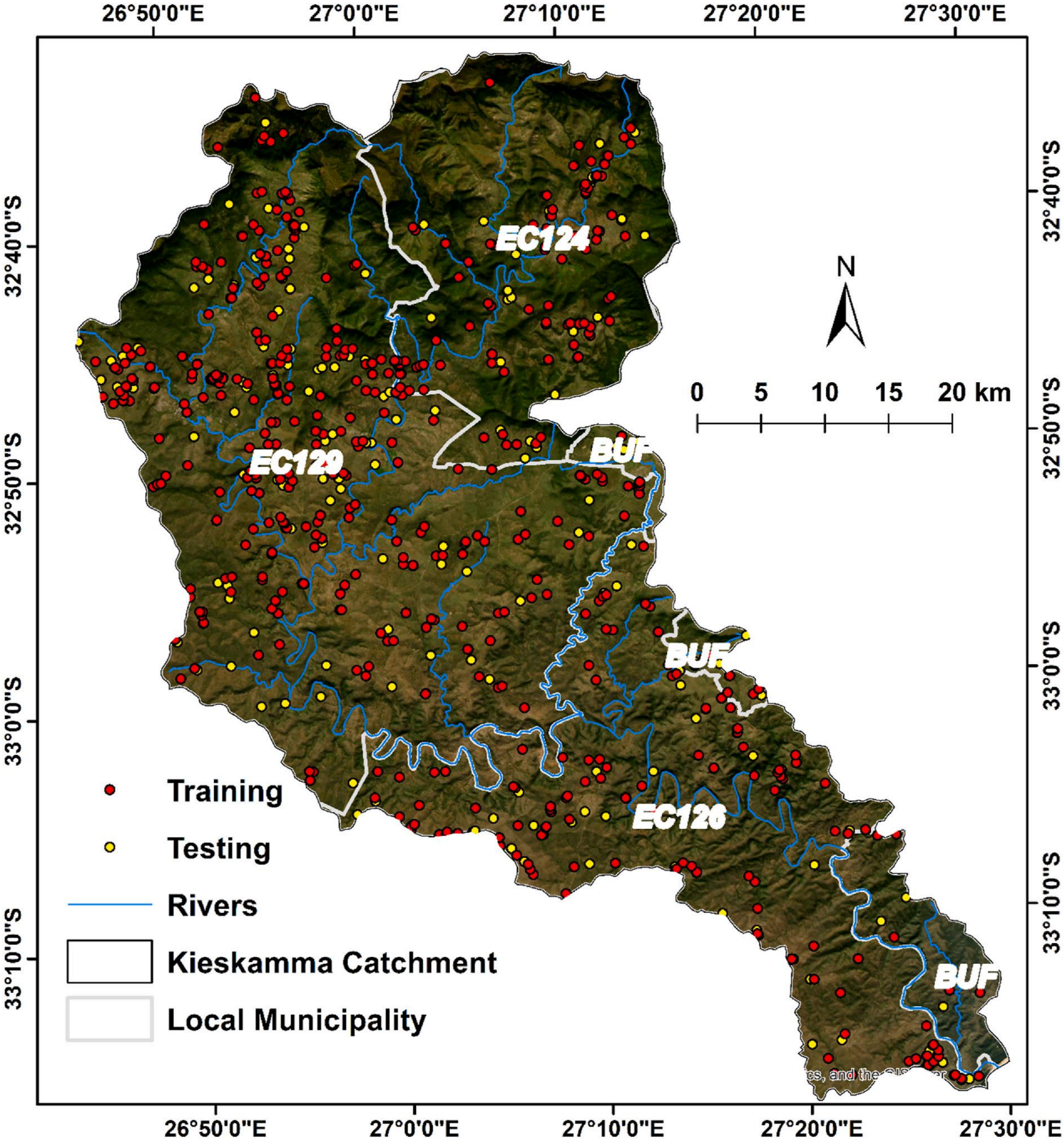

Fig. 2. Training and testing borehole sample groundwater points mapped out on the elevation map of the study area.

tectonic lineaments were used to create a lineament density map using the line density tool of ArcGIS. The land use land cover (LULC) features were determined using Sentinel-2 MSI retrieved from the European Space Agency (ESA) Copernicus Hub (https://scihub.copernicus.eu/). The image was then pre-processed for geometric distortion and atmospheric noise/impurities to enhance the quality of the image in ENVI software. Sentinel data for this study area was classified using support vector machine and ground-truth validation data to map identified land features. The ground-truth data was also used to compute the assessment accuracy of the classified image. To determine the slope and drainage density of the catchment, a 30 m Digital Elevation Model (DEM) was retrieved from the Open Topography platform (https://www.opentopography.org). Soil data were acquired from SORTER (https://files.isric.org/public/soter/SAF-SOTER.zip). A drainage density map was prepared by filling the Shuttle Radar Topography Mission (STRM) DEM, and later used flow direction and flow accumulation in ArcGIS. Vectorization of the raster drainage map was carried out by using conversion tools. Finally, the line density command in ArcGIS was used to compute the drainage density map. The geology of the catchment was retrieved from the existing map of the Geological Survey of South Africa (GSSA) (https://www.gssa.org.za/) using ArcGIS. Rainfall data of the area was retrieved from the South African Weather Services (SAWS) (https://www.weathersa.co.za/), and the inverse distance weighting (IDW) interpolation technique in ArcGIS was used to map rainfall distribution. The schematic framework for the GWPZ characterization and mapping of the Kieskamma Catchment was achieved through the integration of geospatial-based tools, AHP as well as FR approaches (see Fig. 3).

Table 1
Dataset used in this study for groundwater potential zonation mapping.

Data set	Source	Scale	Period	Factors
Landsat 8 OLI	USGS Earth Explorer	30 m	July 9, 2022	Lineament
SRTM DEM	Open Topography	30 m	July 9, 2022	Drainage
Geology	GSSA	1:250 000	1966–2010	Geology
Soil data	SOTERSAF	1:250 000	2004	Soil type
Meteorological data	SAWS	–	2012–2022	Rainfall
Sentinel-2 data	Copernicus Hub	10 m	June 2, 2022	LULC
Borehole	National Groundwater Archive	–	2001–2018	Borehole location

OLI** Operational Land Imager, ***USGS: United States Geological Survey, ***SRTM:*** Shuttle Radar Topography Mission, ***DEM:*** Digital Elevation Model, ***GSSA:*** Geological Survey of South Africa, ***SOTERSAF:*** Soil and Terrain database for South Africa, ***SAWS:*** South African Weather Services, NGA: National Groundwater Archive.

2.3. Integrated computer-aided algorithms for groundwater characterization

2.3.1. Analytical hierarchy process (AHP) model

AHP is a popular MCDM approach for assessing and solving complex decision problems through priority decomposition, comparison judgment, and synthesis (Mondal and Maiti, 2013; Halder et al., 2022). The AHP approach is built on a series of pairwise evaluation matrices (see Equation (1)) that evaluate the weights of each criterion by contrasting inclusive criteria with one another (Tariq et al., 2023; Saaty, 1980). The AHP approach appraises several datasets in a comparison matrix, which is commonly used to measure geometric mean and normalized weight (Majeed et al., 2023). The weights of each various stratum were assigned based on expert knowledge, field experience, and the potential impact of groundwater.

$$A = \begin{bmatrix} a_{11} & a_{12} & \dots a_{1n} \\ a_{21} & a_{22} & \dots a_{2n} \\ a_{n1} & a_{n2} & \dots a_{nn} \end{bmatrix} \quad (1)$$

Where A is the judgment matrix, and a_{nn} is an indicator of the judgment matrix element.

Consistency was computed to detect the logic judgment matrix, class weight, and consistency ratio (CR). CR of a pairwise comparison was then derived using the following expressed Equation (2):

$$CR = \frac{CI}{RI} \quad (2)$$

Where CR is the consistency ratio – which is performed to authenticate the judgment logic, CI is the Consistency Index, and RI is the Random Index (value depends on the order of the matrix). The CI was computed using expressed Equation (3) below:

$$CI = \frac{\lambda_{max} - n}{n - 1} \quad (3)$$

where, λ_{max} is the maximum eigenvalue of A, which signifies the weighted sum to normalized weight ratio, and n is the number of site-specific factors that were employed to analyze the square matrix. As shown in Table 2, the random CI value was computed using Saaty's standard.

2.4. Parameter weighting and pairwise comparison matrix construction

The parameter weights were allocated controlling factors based on their comparative importance to groundwater existence, using expert knowledge (Saaty, 1980). The parameters that notably subsidize groundwater existence were assigned a higher weightage, and parameters that subsidize groundwater less were ranked lower. The parameters and sub-category ranking were carried out based on Saaty's 1–9 scale of relative importance (Saaty, 1980).

2.5. Determination of groundwater potential zone identification

For the determination of GWPZ, the weighted overlay analysis (WOA) tool was utilized to superimpose and reclassify the thematic layers of all selected parameters (Das and Pal, 2019). Each cell value in the input raster was given a score using the evaluation scale. Subsequently, the calculated weights were employed to modify the raster dataset, whereby the cell scores of each input raster were multiplied by the corresponding weighting values assigned to each raster layer as presented in Equation (4):

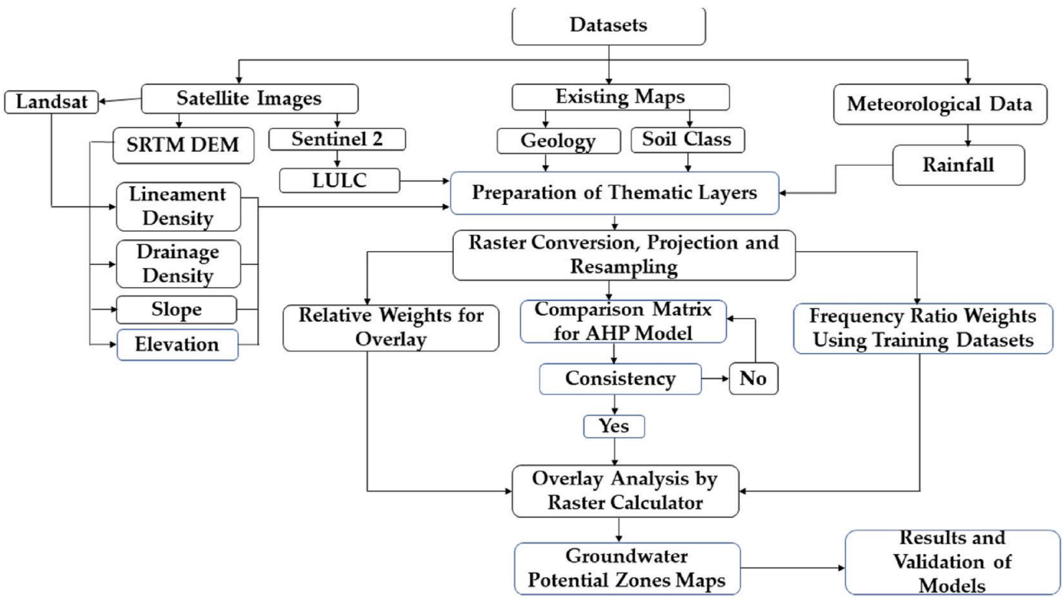

Fig. 3. Conceptual framework of the methodological design undertaken in this study.

Table 2
Matrix of pairwise comparisons and weights of groundwater controlling factors.

Matrix		Rainfall 1	Geology 2	Slope 3	Drainage density 4	LULC 5	Lineament density 6	Soil 7	Weight
Rainfall	1	1	3	3	5	5	5	6	37.87%
Geology	2	1/3	1	3	3	5	4	4	23.65%
Slope	3	1/3	1/3	1	1	3	3	4	12.86%
Drainage density	4	1/5	1/3	1	1	1	2	4	9.63%
LULC	5	1/5	1/5	1/3	1	1	1	3	6.80%
Lineament density	6	1/5	1/4	1/3	1/2	1	1	1	5.23%
Soil	7	1/6	1/4	1/4	1/4	1/3	1	1	3.97%

$$GWPZ = SL_W SL_R + RF_W RF_R + LD_W LD_R + SC_W SC_R + DD_W DD_R + GL_W GL_R + LC_W LC_R \quad (4)$$

where, SL is slope, RF is rainfall, LD is lineament density, SC is soil classification, DD is drainage density, GL is geology and LC is land use/ land cover. The subscripts W represent the weight of each factor, and R is a ranked value (see Table 3) of each groundwater factor, respectively.

2.6. Frequency ratio (FR)

FR was utilized to define the probable GWPZ based on the correlation between independent and dependent variables. FR is the panorama of the occurrence of a certain factor (Kheradmand et al., 2018). The basis of FR is the relationship between the distribution of observational boreholes and the controlling factors related to groundwater potential. FR of a certain factor can easily be computed using the following expression:

Table 3
Ranks assigned for individual subclasses of groundwater controlling factors.

Factors	Sub-class	Rank	Factors	Sub-class	Rank
Geology	Adelaide	5	**Drainage Density (km/km^2)**	0–0.00354	5
	Karoo dolerite	4		0.003538–0.00631	4
	Nanaga	5		0.006311–0.00908	3
	Quaternary	4		0.009084–0.01186	2
	Tarkastad	5		0.011857–0.01463	1
Rainfall (mm)	600–630	4	**Soil**	Lithic Leptosols	2
	630–660	4		Rhodic Ferralsols	5
	660–690	4		Eutric Regosols	3
	690–710	5		Haplic Lixisols	5
	710–730	5		Rhodic Nitisols	4
Lineament Density (km/km^2)	0–0.00058	1		Eutric Leptosols	2
	0.00058–0.00116	2		Eutric Cambisols	4
	0.00116–0.00174	3		Ferric Luvisols	5
	0.00174–0.00232	4		Haplic Luvisols	5
	0.00232–0.00290	5		Dystric Regosols	3
Slope (°)	0–5.28	5		Albic Arenosols	5
	5.29–10.3	4			
	10.4–16.6	3			
	16.7–25.6	2			
	25.7–67.3	1			
LULC	Water	5			
	Trees	3			
	Wetland	5			
	Crops	3			
	Built-up area	1			
	Bare land	2			
	Range land	1			

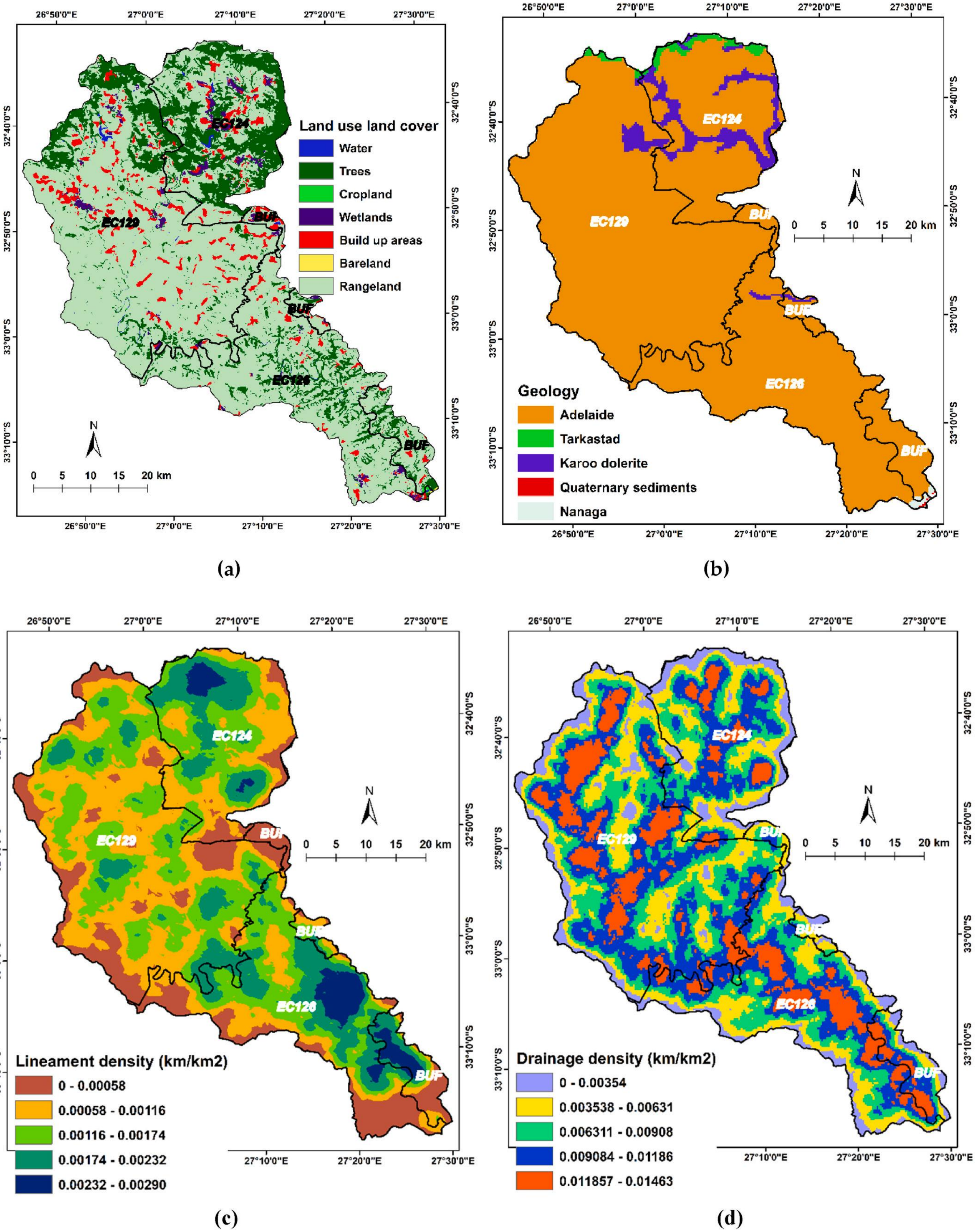

Fig. 4. Controlling factors used in this study to prepare GWPZ maps: (a) Land use/land cover, (b) Geology, (c) Lineament density, (d) Drainage density, (e) Slope, (f) Soil class and (g) Rainfall.

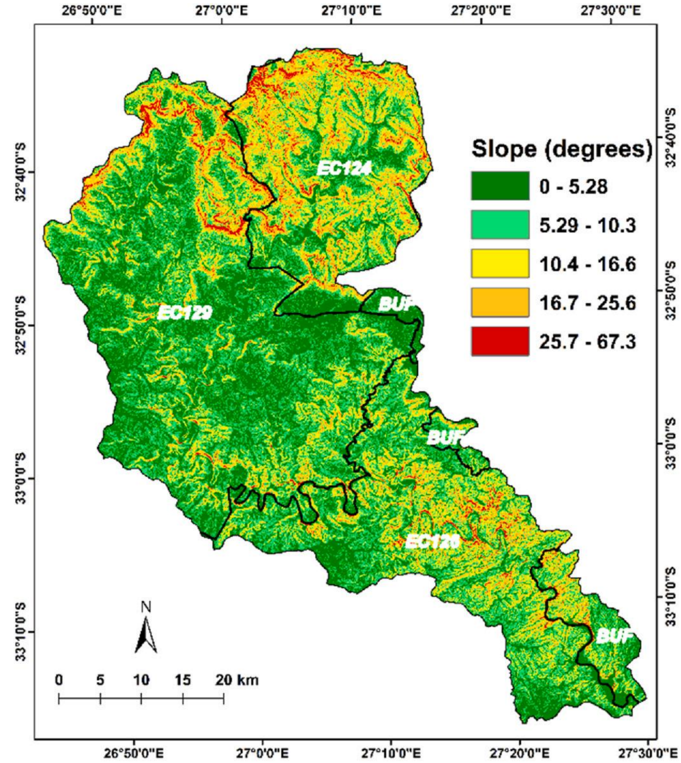

(e)

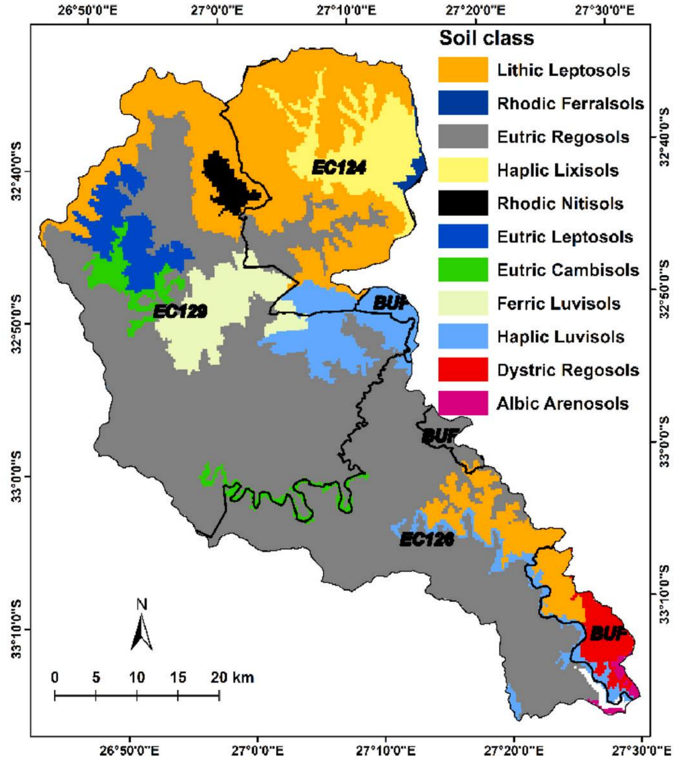

(f)

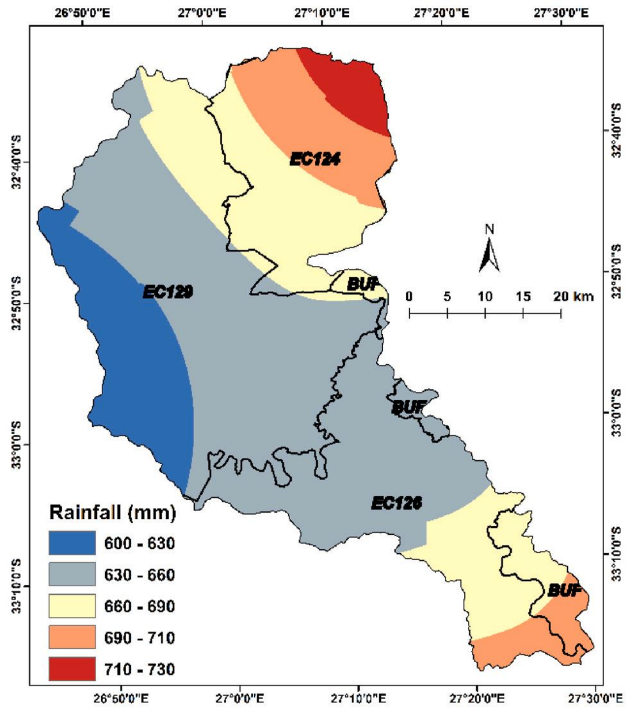

(g)

Fig. 4. (*continued*).

$$FR = \left[\frac{\left(\frac{P_{gw}}{T_{gw}}\right)}{\left(\frac{P_j}{T_j}\right)}\right] = \left[\frac{\%\ boreholes}{\%\ pixels}\right] \tag{5}$$

Where, P_{gw} is the number of pixels with wells for each parameter, T_{gw} is the number of total wells, P_j is the number of pixels in the classes of a parameter, T_j is the total number of pixels of a parameter (Table 1).

The FR values were further normalized in a range of probability values (0–1) as relative frequency (RF) using Equation (6) below:

$$RF = \frac{FR}{Sum\ (FR)} \tag{6}$$

To find a mutual interrelation among contributory factors, a weight or predictor rate (PR) was calculated by rating each contributory factor with the training dataset of boreholes using Equation (7).

$$PF = \frac{MaxRF - Min\ RF}{(Max - Min)MinRF} \tag{7}$$

2.7. Validation and accuracy assessment for AHP and FR models

To validate the reliability of the GWPZ, 784 boreholes were classified into two categories (training and testing) and were mapped out. The sample points are used to estimate the area under the curve (AUC) of the receiver operating characteristic (ROC). To estimate the effectiveness of AHP and FR models, true negative, false positive, and true positive results were integrated to generate the ROC curve and the AUC. These parameters will calculate 1-specificity and sensitivity. The sensitivity (Equation (8)) is the proportion of correctly classified groundwater potential pixels, while specificity (Equation (9)) is the proportion of correctly classified non-groundwater potential pixels. Equation (10) is used to compute the AUC, which ranges from 0.5 to 1. The AUC values are evaluated as follows: excellent (0.9–1), very good (0.8–0.9), good (0.7–0.8), moderate (0.6–0.7), and poor (0.5–0.6) (Fawcett, 2006). The ArcSDM toolbox embedded in ArcGIS 10.8 software was used to generate the AUC values.

$$\text{Sensitivity} = \frac{\text{TP}}{\text{TP} + \text{FN}} \tag{8}$$

$$\text{Specificity} = \frac{\text{TN}}{\text{TN} + \text{FP}} \tag{9}$$

$$\text{AUC} = \frac{\sum \text{TP} + \sum \text{TN}}{\text{n}} \tag{10}$$

Where, TP signifies true positive, TN for true negative, FP for false positive, FN for false negative, and n denotes groundwater source pixel as well as the equivalent number of non-groundwater potential pixels.

2.8. Boreholes

In this study, a total of 784 boreholes were retrieved from a National Groundwater Archive (NGA). These sample points were randomly subdivided into two categories (532 training boreholes and 252 testing boreholes; see Fig. 2) using the subset feature technique of the geospatial analyst tool in ArcGIS.

3. Results

3.1. Controlling factors used to assess GWPZs

Keiskamma Catchment is dominated by several LULC feature types (Fig. 4a), including water (0.49%), trees (27.71%), cropland (1.85%), wetlands (0.07%), built-up (5.98%), bareland (0.03%), and rangeland (63.88%). Rangeland and tree cover occupy a large proportion of the environment across the rugged terrain of the catchment. The classified map of the area using the Sentinel dataset achieved an overall accuracy of 89%.

The geology map (Fig. 4b) (Table 5) shows that the Keiskamma Catchment is composed of Adelaide Supergroup (94.07%), Karoo dolerite (4.53%), Tarkastad Supergroup (1.13%), Nanaga Formation (0.22%), and Quaternary sediments (0.04%). The Adelaide and Tarkastad Supergroups of the Beaufort Group are composed of sedimentary rocks (sandstones, mudstones, and shale) which are intruded by Karoo dolerites (dykes and sills). The Nanaga Formation also consists of sandstones. The Quaternary sediments are found near the sea coast.

Fig. 4c depicts the lineament density of faults, fractures, and joints, which can promote recharge, aquifer storage, and groundwater flow. Five (5) subclasses occupy roughly 30.60%, 53.62%, 13.60%, 1.76%, and 0.42% of the total surface area, as depicted in Fig. 4c. The lineament density map reveals that the center area of the study region exhibits the most pronounced concentration of lineaments. The southern and northwestern regions exhibit varying degrees of lineament density, ranging from moderate to high levels. The eastern portion of the research zone exhibits a very low density of lineaments. According to the data presented in Table 3, the lineament density class with the highest value in terms of kilometers per square kilometer obtained the highest rank of 5. Conversely, the lineament density class with the lowest value received the lowest rank of 1.

The drainage density was utilized to estimate the length of all orders in the catchment area. In the Keiskamma catchment, drainage density ranges from 0 to 0.01463 km/km^2 (Fig. 4d). This drainage density map was reclassified using Jenks natural breaks classification into five categories, namely very low (0–0.00354 km/km^2)(10.24%), low (0.003538–0.00631 km/km^2)(21.48%), moderate (0.006311–0.00908 km/km^2)(25.04%), high (0.009084–0.01186 km/km^2)(27.49%), and very high (0.011857–0.01463 km/km^2)(15.76%) and this results indicate that majority of the catchment fit in to moderate and high drainage density class.

The slopes of the Keiskamma catchment range from 0 to 67.3° (Fig. 4e). The upstream and the mid-lower streams have steep slopes, but the mid-stream, northwestern, and southwestern regions of the catchment have gentle undulating flat areas. The slopes were reclassified into five classes, i.e., very gentle $<5.28^\circ$ (69.43%), gentle 5.29–10.30° (29.12%), moderate 10.4–16.60° (1.32%), steep 16.7–25.60° (0.13%) and very steep slope, 25.70–67.30° (0.01%). Areas with very gentle and gentle slopes exhibit a high potential for groundwater availability.

The soils of the area belong to eleven regional level-2 reference soil groups, including Lithic Leptosols, Rhodic Ferralsols, Eutric Regosols, Haplic Lixisols, Rhodic Nitisols, Eutric Leptosols, Eutric Cambisols, Ferric Luvisols, Haplic Luvisols, Dystric Regosols, and Albic Arenosols, which exhibit significant differences in their soil properties (Table 4). As shown in Table 3, the Rhodic Ferralsols, Haplic Lixisols, Ferric Luvisols, Haplic Luvisols, and Albic Arenosols rank the highest for groundwater potential, but all are of limited extent in the catchment. The soil map of the catchment (Fig. 4f) shows that Eutric Regosols (55.03%) and Lithic Leptosols (21.95%) dominated the study area but are ranked 3 and 2, respectively, related to groundwater potential (see Table 6).

The mean annual rainfall of the study area (Fig. 4g) was classified

Table 4
Explanation of soil types present in the catchment.

Soil class	Description
Lithic Leptosols	Very shallow rocks with limited soil developments
Rhodic Ferralsols	Deep, strongly weathered upland soils, well developed soils
Eutric Regosols	Soils with very limited soil development
Haplic Lixisols	Upland soils mostly well-developed soils
Rhodic Nitisols	Dark red, mostly well-developed clayey soils
Eutric Leptosols	Very shallow rocks with limited soil developments
Eutric Cambisols	Weakly to moderately developed soils; Soils with no or little soil developments
Ferric Luvisols	Well-developed soils with subsurface accumulation of high activity clays and high base saturation
Haplic Luvisols	Well-developed soils with subsurface accumulation of high activity clays and high base saturation
Dystric Regosols	Soils with very limited soil development
Albic Arenosols	Loamy sandy soils featuring well developed soils

Table 5
Explanation of geology types present in the catchment.

Geology type	Description
Adelaide	It forms the lower part of the Beaufort Group in the Karoo Supergroup. It comprises medium to fine-grained sandstones and greenish-to-reddish mudstones.
Karoo dolerite	It comprises interconnected networks of dykes and sills, which are the common types of intrusion in the Karoo Basin.
Nanaga	It belongs to the Algoa Group of the Karoo Supergroup, which comprises semi-consolidated and cross-bedded sandstones and sandy limestones.
Quaternary	These sediments have good variable textures (gravel, clay, sand, and silt), hydraulic conductivities, and porosities.
Tarkastad	It forms the upper part of the Beaufort Group in the Karoo Supergroup. It consists of red and maroon mudstones and fine to medium-grained grey sandstone.

using the Jenks natural breaks classification method into five subclasses: very low (600–630 mm), low (630–660 mm), moderate (660–690 mm), high (690–710 mm), and very high (710–730 mm), occupying about 12.12%, 48.62%, 25.15%, 11.39%, and 2.73% of the total catchment area, respectively. Table 3 shows the ranks associated with these subclasses.

3.2. Groundwater potential zonation (GWPZ) maps derived from AHP and FR

The weights derived using the AHP and FR models were utilized to delineate the GWPZs of Keiskamma Catchment (Fig. 5a and b) (see Table 6). The spatially distributed GWPZs of the catchment derived using AHP were reclassified into five categories (Table 7) of varying groundwater potentials, i.e., very low, low, moderate, high, and very high. In the catchment, approximately 3640.743 km^2 was classified as a

Table 6
Ranks (RF) and weights (PR) assigned to subclasses and factors to determine GWPZs using FR.

Factor	Class	Class Pixels %	Geosite Pixels %	FR	RF	MinRF	MaxRF	Max-Min RF	(Max-Min) MinRF	PR
Geology	Adelaide	94.07819	96.21928	1.02276	0.07719					
	Karoo dolerite	4.53003	0.18904	0.04173	0.00315					
	Nanaga	0.21975	2.45747	11.18277	0.84398					
	Quaternary	0.03855	0	0	0					
	Tarkastad	1.13347	1.13422	1.00066	0.07552					
Total		**100**	**100**	**13.247912**	**1**	**0**	**0.84398**	**0.84398**	**0.17607**	**4.79355**
Rainfall (mm)	600–630	12.11675	15.41353	1.27208	0.28371					
	630–660	48.62207	54.32331	1.11726	0.24918					
	660–690	25.14912	19.36090	0.76984	0.17169					
	690–710	11.38582	9.58647	0.84197	0.18778					
	710–730	2.72624	1.31579	0.48264	0.10764					
Total		**100**	**100**	**4.48379**	**1**	**0.10764**	**0.28371**	**0.17607**	**0.17607**	**1**
Lineament Density (km/km^2)	0–0.00058	30.60344	15.22556	0.49751	0.02932					
	0.00058–0.00116	53.61932	34.02256	0.63452	0.03739					
	0.00116–0.00174	13.59637	33.83459	2.48850	0.14664					
	0.00174–0.00232	1.76062	14.84962	8.43431	0.49701					
	0.00232–0.00290	0.42025	2.06767	4.92012	0.28993					
Total		**100**	**100**	**16.97496**	**1**	**0.02932**	**0.49701**	**0.46770**	**0.17607**	**2.65636**
Slope (°)	0–5.28	36.90716	94.92481	2.57199	0.93868					
	5.29–10.3	33.13396	4.88722	0.14750	0.05383					
	10.4–16.6	18.29590	0	0	0					
	16.7–25.6	9.17105	0.18797	0.02050	0.0074803					
	25.7–67.3	2.49193	0	0	0					
Total		**100**	**100**	**2.7399836**		**0**	**0.938682**	**1**	**0.17607**	**5.67968**
LULC	Water	0.48676	0.18797	0.38617	0.06310					
	Trees	27.70897	10.33835	0.37310	0.06096					
	Wetlands	0.07162	0	0	0					
	Crops	1.84822	2.81955	1.52555	0.24927					
	Built-up area	5.98011	16.35338	2.73463	0.44683					
	Bare land	0.02923	0	0	0					
	Rangeland	63.87509	70.30075	1.10060	0.17983					
Total		**100**	**100**	**6.12005**		**0**	**0.446831**	**0.44683**	**0.17607**	**2.53786**
Soil Class	Lithic Leptosols	21.95072	8.46154	0.38548	0.03160					
	Rhodic Ferralsols	0.34454	0	0	0					
	Eutric Regosols	53.03322	55.96154	1.05522	0.08649					
	Haplic Lixisols	5.11520	5.96154	1.16546	0.09553					
	Rhodic Nitisols	0.96777	0.38462	0.39742	0.03258					
	Eutric Leptosols	3.14346	5.57692	1.77413	0.14542					
	Eutric Cambisols	2.44861	4.03846	1.64929	0.13519					
	Ferric Luvisols	4.49778	11.92308	2.65088	0.21729					
	Haplic Luvisols	6.53269	6.73077	1.03032	0.08445					
	Dystric Regosols	1.66279	0.38462	0.23131	0.01896					
	Albic Arenosols	0.30323	0.57692	1.90262	0.15595					
Total		**100**	**100**	**12.24213**	**1.00345**	**0**	**0.217285**	**0.21729**	**0.17607**	**1.23411**
Drainage Density (km/km^2)	0–0.00354	10.24074	7.90960	0.77237	0.16091					
	0.003538–0.00631	21.47748	19.77401	0.92069	0.19181					
	0.006311–0.00908	25.03774	30.13183	1.20346	0.25072					
	0.009084–0.01186	27.48758	28.62524	1.04139	0.21696					
	0.011857–0.01463	15.75646	13.55932	0.86056	0.17928					
Total		**100**	**100**	**4.79845**	**0.99968**	**0.16091**	**0.999678**	**0.83877**	**0.17607**	**4.76393**

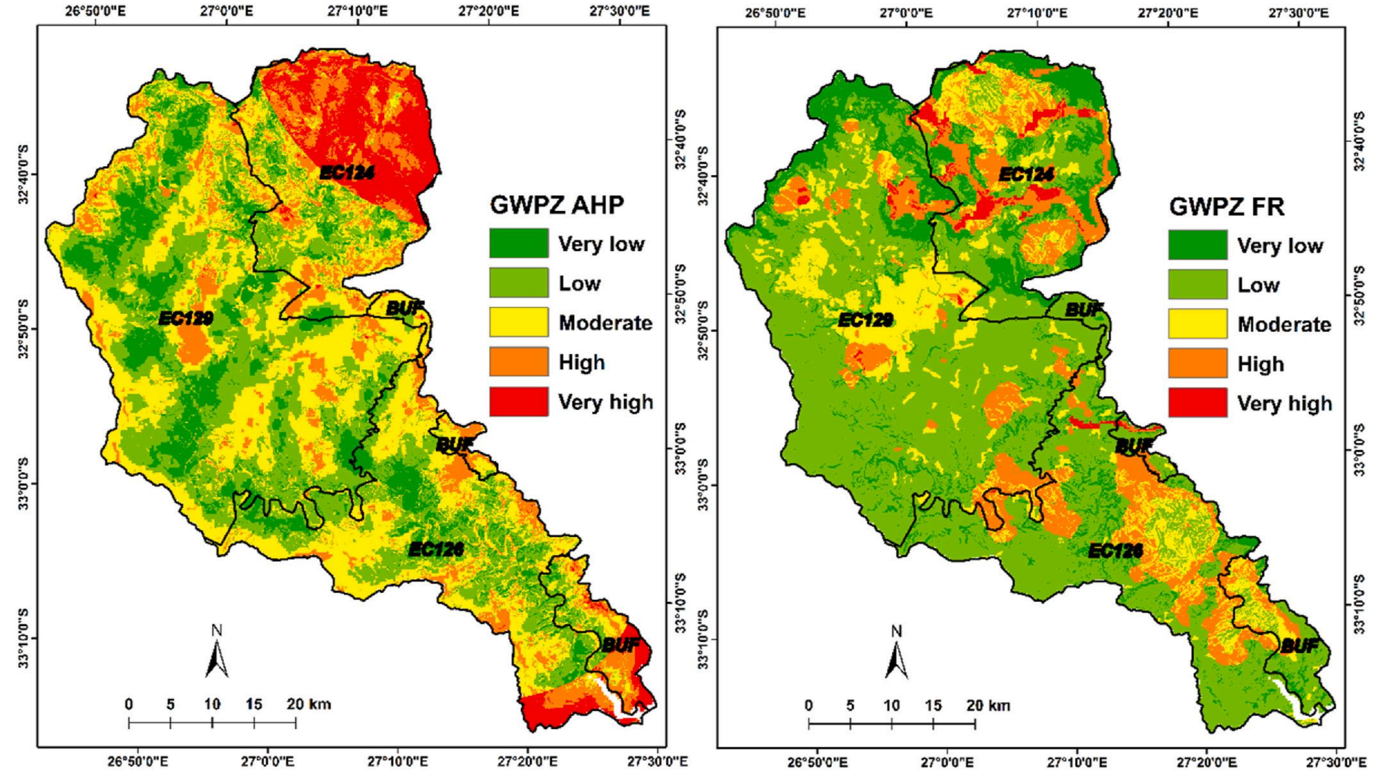

Fig. 5. GWPZ maps computed by (a) AHP and (b) FR.

very low potential zone, and it accounted for roughly 13.59% of the total area of the catchment. Low (8029.47 km^2) and moderate (8825.62 km^2) potential zones occupy 29.98% and 32.96% of the total area, respectively. High (4029.85 km^2) and very high (2254.78 km^2) potential zones cover respective extents of 15% and 8.42%. When using FR, five categories were also reclassified. In the catchment, approximately 3886.50 km^2 was classified as a very low potential zone, accounting for roughly 14.51% of the extent area of the catchment. Low (967.91 km^2) and moderate (17 602.34 km^2) potential zone occupy 3.61% and 65.73% of the total area, respectively. High (3847.97 km^2) and very high (475.75 km^2) potential zones account for only 14.37% and 1.78% of the catchment area.

3.3. Model performance validation

In this study, the GWPZ characterization maps were evaluated using the bivariate correlation between the controlling factors and boreholes, and AUC was utilized to evaluate the mapping accuracy. The ROC curve results are presented in Fig. 6. These results revealed that FR (AUC = 62%) outperformed AHP (AUC = 50%).

4. Discussion

In this study, geospatial-based AHP and FR models were employed to characterize GWPZs using seven controlling factors (slope, geology, land use land cover, lineaments, drainage density, rainfall, and soil types) and borehole locations. These models have various strategies to weigh the controlling factors. For instance, the FR weights were allocated based on data analysis, but the AHP weights were determined using a decision system approach and expert knowledge.

Based on our analysis, the maps revealed that the spatial distribution of GWPZs is significantly related to soil types. Moreover, the permeable rock structures enable groundwater percolation to recharge groundwater. The recharging potential of lithosols is enhanced when sand, silt, and clay are present in similar amounts (Luo et al., 2023). The coarse texture of soil characteristics increases the aquifer recharge potentiality. The soil types with the most gravel and sand content promote infiltration and recharge as a result of high soil porosity (Luo et al., 2023). As a result, the volume and flow of groundwater in a specific area are influenced by the soil properties of the area under question. Soil controls the infiltration rate and groundwater recharge capabilities as well as influencing lateral flow (Luo et al., 2023). The lithological units of amorphous and heterogeneous sedimentary rocks are primarily found in the very good and good GWPZ. This signifies that the most promising regions for groundwater potential are those where such lithological units predominate.

Prolonged periods of drought have a direct impact or influence on the accessibility and dependence on groundwater, which is attributed to heightened fluctuation in rainfall patterns and intensified weather phenomena resulting from climate variability (Doke et al., 2021). In this study, GWPZ was highest in the northern and southeastern parts of the catchment, where rainfall was high, ranging from 690 to 710 mm in the former and 710–730 mm in the latter, using the AHP algorithm. These areas, particularly the southeastern parts of the catchment, are mainly flat, which probably enhances groundwater recharge.

Aquifer depletion is a phenomenon that is more prone to occur during prolonged periods of drought, especially in aquifers that are tiny and shallow (Bierkens and Wada, 2019). Individuals residing in regions susceptible to drought heavily depend on groundwater due to its

Table 7
Area and percentage of GWPZ level.

	FR		AHP	
	Area	Percent	Area	Percent
Very low	3886.497	14.51	3640.74	13.59
Low	967.905	3.61	8029.47	29.98
Moderate	17602.34	65.73	8825.62	32.96
High	3847.968	14.37	4029.85	15.05
Very high	475.749	1.78	2254.78	8.42

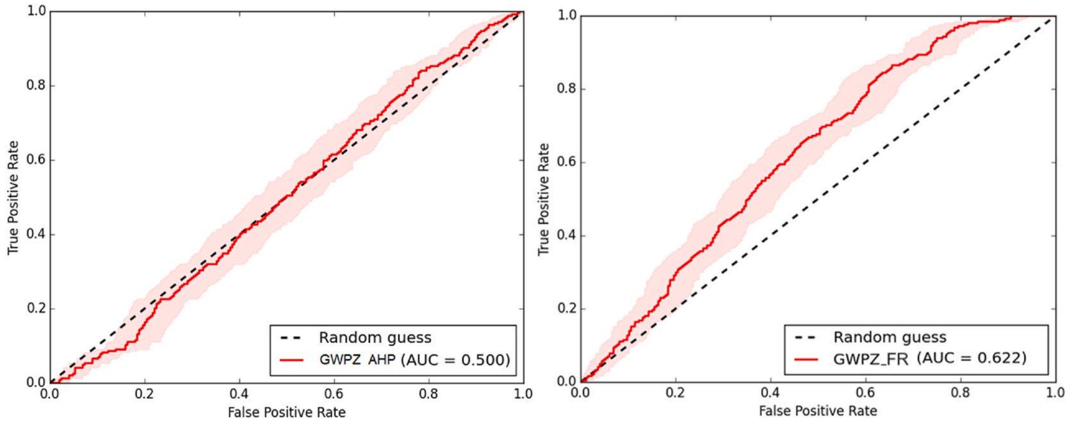

Fig. 6. Validation curve identified and delineated GWPZ using (a) GWPZ_AHP and (b) GWPZ_FR. The area under the curve (a) is 0.500 (50%) and (b) is 0.622 (62%), which is the accuracy of the delineated GWPZ map.

capacity to serve as a protective measure (Khan et al., 2023). Considering the intricate spatial dynamics of factors influencing groundwater vulnerability (Baalousha and Lowry, 2022), it is imperative to acknowledge and integrate causal components within a comprehensive framework. GWPZ modeling is now regarded as a vastly effective approach for assessing and managing groundwater (Sherif et al., 2023). Groundwater recharge has significantly decreased due to various activities (human and environmental) as well as imbalanced development (Shekar and Mathew, 2023). Characterizing GWPZ hotspots within drought-prone areas can benefit groundwater usage and sustainable management, as well as the establishment of artificial groundwater recharge structures.

The estimated performance of the models in characterizing GWPZs revealed that FR (AUC = 62%) produced superior results compared to AHP (AUC = 50%). These findings align with previous studies by Uvaraj (2021) and Muavhi et al. (2022), which reported that the FR model is more reliable for predicting groundwater potential than the AHP model. For instance, work done by Uvaraj (2021) showed that FR (AUC = 68.5%) outperformed the AHP (AUC = 41.1%) selective and knowledge-based influencing factor model. Contrarily, Mukherjee and Singh (2020) and Ikirri et al. (2023) studies revealed a good predictive accuracy of the AHP model with AUC of 71.50% and 80%, respectively.

To implement precise, timely initiatives to control groundwater withdrawal and alleviate water shortages, it is essential to comprehend the relationship between GWPZ occurrences and controlling factors. In regions that are prone to drought, it is imperative to use a synergistic approach that combines remote sensing and geospatial approaches to understand the status of groundwater. This approach is essential for implementing a range of preventive interventions aimed at addressing potential groundwater occurrences while also ensuring environmental preservation and long-term sustainability (Ghanim et al., 2023). The derived thematic maps of the controlling factors will support research and development of advanced technologies and strategies, as well as collaboration amongst hydrogeological experts, to enhance planning, decision-making, rural infrastructure development, and implementation of groundwater depletion mitigation measures.

4.1. Limitation of the study

The variations in the AUC values of the AHP model could be attributed to the weight allocated to each groundwater controlling factor, which depends on the expert's knowledge. According to Chowdary et al. (2013), the total dependency on the expert's opinion is the main source of uncertainty in the AHP model since insufficient judgment on a factor can poorly influence the assigned weight. The resultant GWPZ maps from the AHP and FR models are subjected to other limitations. For instance, the digital elevation model (DEM) and Landsat 8 OLI satellite imagery used in this study are of medium resolution of 30 × 30 m. Echogdali et al. (2023) alluded that the spatial resolution of the input data directly impacts the model outcomes. Hence, it is advisable to employ higher-resolution input data to improve the accuracy of the resulting GWPZ map (El Ayady et al., 2023). Additionally, the random classification of borehole data during training and testing processes may introduce considerable uncertainty in GWPZ mapping (Aswathi et al., 2022; El Ayady et al., 2023). However, the AUC values from both models (AHP and FR) used in this research exceed the minimum acceptable AUC value of 50% (Fawcett 2006).

5. Conclusions

The GWPZs in the Keiskamma Catchment of South Africa were characterized using geospatial-based (AHP and FR) models, remote sensing techniques, and geographic information system (GIS) techniques. To achieve this, seven maps of controlling factors such as slope, geology, rainfall, drainage density, soil, lineaments, and land use land cover were used to characterize GWPZ in a GIS environment. The outcome of this study showed that combining diverse geospatial datasets from various sources is a significant instrument for detecting and investigating groundwater in water-scarce environments. The estimated performance of the models revealed that FR (AUC = 62%) produced superior results compared to AHP (AUC = 50%) in characterizing GWPZs. The AHP-derived high to very high prospective zones are situated in northeast headwater areas and near the mouth of the catchment, but the FR-derived high zones are of a larger extent and cover a greater proportion of the lower catchment. The study demonstrated the usefulness of FR in characterizing GWPZs in water-scarce regions. Studies in other regions with the same climatological, geomorphological, and water shortage conditions can adopt a similar approach to advance the characterization of GWPZ for sustainable groundwater management. Also, hybrid models can be integrated to assist policymakers and water-related scientists/managers in enhancing management strategies as well as policies, especially in water-scarce regions.

CRediT authorship contribution statement

Kgabo Humphrey Thamaga: Writing – review & editing, Writing – original draft, Visualization, Validation, Supervision, Software, Resources, Project administration, Methodology, Investigation, Funding acquisition, Formal analysis, Data curation, Conceptualization. **Sinesipho Gom:** Writing – review & editing, Writing – original draft, Methodology, Formal analysis, Data curation, Conceptualization. **Gbenga Olamide Adesola:** Validation, Software, Project administration, Methodology, Investigation, Formal analysis, Data curation, Conceptualization. **Naledzani Ndou:** Writing – review & editing, Validation, Resources. **Nndanduleni Muavhi:** Writing – review & editing, Writing – original draft, Supervision, Methodology, Formal analysis, Conceptualization. **Mthunzi Mndela:** Writing – review & editing. **Phila Sibandze:** Writing – original draft, Validation, Formal analysis. **Hazem Ghassan Abdo:** Writing – review & editing, Methodology. **Thabang Maphanga:** Writing – review & editing. **Gbenga Abayomi Afuye:** Writing – review & editing. **Benett Siyabonga Madonsela:** Writing – review & editing, Investigation. **Hussein Almohamad:** Writing – review & editing.

Declaration of competing interest

The authors declare that they have no known competing financial interests or personal relationships that could have appeared to influence the work reported in this paper.

Data availability

Data will be made available on request.

Acknowledgments

The authors would like to thank the University of Fort Hare, and the Department of GIS and Remote Sensing for creating and enabling the environment for research.

References

Abdo, H.G., Vishwakarma, D.K., Alsafadi, K., et al., 2024. GIS-based multi-criteria decision making for delineation of potential groundwater recharge zones for sustainable resource management in the Eastern Mediterranean: a case study. Appl. Water Sci. 14, 160. https://doi.org/10.1007/s13201-024-02217-z.

Adesola, G.O., Thamaga, K.H., Gwavava, O., Pharoe, B.K., 2023a. Groundwater potential zones assessment using geospatial models in semi-arid areas of South Africa. Land 12, 1877. https://doi.org/10.3390/land12101877.

Adesola, G.O., 2024. Modeling of groundwater productivity in the Alfred Nzo District, South Africa, using relative frequency ratio and Shannon entropy models. J. Hydrol. Reg. Stud. 54 (2024), 101877. https://doi.org/10.1016/j.ejrh.2024.101877.

Adesola, G.O., Gwavava, O., Liu, K., 2023b. Hydrological evaluation of the groundwater potential in the fractured karoo aquifer using magnetic and electrical resistivity methods: case study of the balfour formation, alice, South Africa. International Journal of Geophysics, 1891759. https://doi.org/10.1155/2023/1891759.

Ait Haddou, M., Bouchriti, Y., Ikirri, M., Wanaim, A., Aydda, A., Amarir, S., et al., 2023. Delineation of groundwater potential zones in a semi-arid region using remote sensing and GIS: a case study of argana corridor (Morocco). In: In Advanced Technology for Smart Environment and Energy. Springer International Publishing, Cham, pp. 257–268.

Aswathi, J., Sajinkumar, K.S., Rajaneesh, A., Oommen, T., Bouali, E.H., Binoj Kumar, R. B., Rani, V.R., Thomas, J., Thrivikramji, K.P., Ajin, R.S., Abioui, M., 2022. Furthering the precision of RUSLE soil erosion with PSInSAR data: an innovative model. Geocarto Int. 37 (27), 16108–16131.

Baalousha, H.M., Lowry, C.S., 2022. Applied groundwater modelling for water resource management and protection. Water 14, 1142. https://doi.org/10.3390/w14071142.

Basson, W., 2012. From science to society-finding innovative solutions towards deep rural water supply. Water Wheel 11 (6), 32–35.

Bierkens, M.F.P., Wada, Y., 2019. Non-renewable groundwater use and groundwater depletion: a review. Environ. Res. Lett. 14, 063002 https://doi.org/10.1088/1748-9326/ab1a5f.

Boretti, A., Rosa, L., 2019. Reassessing the projections of the World water development report. NPJ Clean Water 2, 15. https://doi.org/10.1038/s41545-019-0039-9.

Busico, G., Giuditta, E., Kazakis, N., Colombani, N.A., 2019. Hybrid GIS and AHP approach for modeling actual and future forest fire risk under climate change accounting water resources attenuation role. Sustainability 11, 7166. https://doi.org/10.3390/su11247166.

Chowdary, V.M., Chakraborthy, D., Jeyaram, A., Murthy, Y.K., Sharma, J.R., Dadhwal, V.K., 2013. Multi-criteria decision making approach for watershed prioritization using analytic hierarchy process technique and GIS. Water Resour. Manag. 27, 3555–3571.

Dar, T., Rai, N., Bhat, A., 2021. Delineation of potential groundwater recharge zones using analytical hierarchy process (AHP). Geology, Ecology and Landscapes 5, 292–307. https://doi.org/10.1080/24749508.2020.1726562.

Das, B., Pal, S.C., 2019. Combination of GIS and fuzzy-AHP for delineating groundwater recharge potential zones in the critical Goghat-II block of West Bengal, India. Hydro. Research 2, 21–30. https://doi.org/10.1016/j.hydres.2019.10.001.

Das, S., Pardeshi, S.D., 2018. Integration of different influencing factors in GIS to delineate groundwater potential areas using IF and FR techniques: a study of Pravara basin, Maharashtra, India. Appl. Water Sci. 8, 1–16. https://doi.org/10.1007/s13201-018-0848-x.

Das, S., Gupta, A., Ghosh, S., 2017. Exploring groundwater potential zones using MIF technique in a semi-arid region: a case study of Hingoli district, Maharashtra. Spatial Information Research 25, 749–756. https://doi.org/10.1007/s41324-017-0144-0.

Doke, A.B., Zolekar, R.B., Patel, H., Das, S., 2021. Geospatial mapping of groundwater potential zones using multi-criteria decision-making AHP approach in a hard rock basaltic terrain in India. Ecol. Indicat. 127, 107685 https://doi.org/10.1016/j.ecolind.2021.107685.

Dondo, C., Woodford, A.C., Murray, R., Nhleko, L.O., Gqiba, D., Chevallier, L., 2010. Flow conceptualisation, recharge and storativity determination in karoo aquifers, with special emphasis on Mzimvubu Keiskamma and Mvoti-Umzimkulu water management areas in the Eastern Cape and Kwazulu-Natal provinces of South Africa. WRC Report, (1565/1/10).

Echogdali, F.Z., Boutaleb, S., Bendarma, A., Saidi, M.E., Aadraoui, M., Abioui, M., Ouchchen, M., Abdelrahman, K., Fnais, M.S., Sajinkumar, K.S., 2022. Application of analytical hierarchy process and geophysical method for groundwater potential mapping in the Tata basin, Morocco. Water 14 (15), 2393.

Echogdali, F.Z., Boutaleb, S., El Ayady, H., Aadraoui, M., Abdelrahman, K., Bendarma, A., Ikirri, M., Abu-Alam, T., Id-Belqas, M., Abioui, M., 2023. Characterization and productivity of alluvial aquifers in sustainability oasis areas: a case study of the Tata watershed (southeast Morocco). Appl. Sci. 13 (9), 5473. https://doi.org/10.3390/app13095473.

Edokpayi, J.N., Rogawski, E.T., Kahler, D.M., Hill, C.L., Reynolds, C., Nyathi, E., Smith, J.A., Odiyo, J.O., Samie, A., Bessong, P., Dillingham, R., 2018. Challenges to sustainable safe drinking water: a case study of water quality and use across seasons in rural communities in Limpopo Province, South Africa. Water 10 (2), 159.

El Ayady, H., Mickus, K.L., Boutaleb, S., El Morjani, Z.E.A., Ikirri, M., Echogdali, F.Z., Bessa, A.Z.E., Abdelrahman, K., Id-Belqas, M., Essoussi, S., Fnais, M.S., 2023. Investigation of groundwater potential using geomatics and geophysical methods: case study of the Anzi sub-basin, western Anti-Atlas, Morocco. Adv. Space Res. 72 (9), 3960–3981.

Fawcett, T., 2006. An introduction to ROC analysis. Pattern Recog Lett 27, 861–874. https://doi.org/10.1016/j.patrec.2005.10.010.

Ghanim, A.A.J., Al-Areeq, A.M., Benaafi, M., Al-Suwaiyan, M.S., Aghbari, A.A.A., Alyami, M., 2023. Mapping groundwater potential zones in the habawnah basin of southern Saudi arabia: an AHP- and GIS-based approach. Sustainability 15, 10075. https://doi.org/10.3390/su151310075.

Greckschlack, K., 2015. Adaptive capacity and water governance in the Keiskamma River catchment, Eastern Cape province, South Africa. WaterSA 41 (3), 359–368.

Halder, B., Banik, P., Almohamad, H., Al Dughairi, A.A., Al-Mutiry, M., Al Shahrani, H.F., Abdo, H.G., 2022. Land suitability investigation for solar power plant using GIS, AHP, and multi-criteria decision approach: a case of megacity Kolkata, West Bengal, India. Sustainability 14, 11276. https://doi.org/10.3390/su141811276.

Hwang, C., Yoon, K., 1981. Multiple Attribute Decision Making: Methods and Applications, A State of the Art Survey, vol 11. Sprinnger-Verlag, New York, NY. https://doi.org/10.1007/978-3-642-48318-9.

Ikirri, M., Boutaleb, S., Ibraheem, I.M., Abioui, M., Echogdali, F.Z., Abdelrahman, K., Id-Belqas, M., Abu-Alam, T., El Ayady, H., Essoussi, S., Faik, F., 2023. Delineation of groundwater potential area using an AHP, remote sensing, and GIS techniques in the Ifni Basin, Western Anti-Atlas, Morocco. Water 15 (7), 1436.

Johnson, M.R., Van Vuuren, C.J., Visser, J.N.J., Cole, D.I., Wickens, H.D.V., Christie, A.D. M., Roberts, D.L., 1997. The foreland Karoo basin, South Africa. In: Selley, R. (Ed.), African Sedimentary Basins of the World, vol. 3. Elsevier, Amsterdam, The Netherlands, pp. 269–317, 1997.

Karimi-Rizvandi, S., Goodarzi, H.V., Afkoueieh, J.H., Chung, I.M., Kisi, O., Kim, S., Linh, N.T.T., 2021. Groundwater-potential mapping using a self-learning Bayesian network model: a comparison among metaheuristic algorithms. Water 13, 658. https://doi.org/10.3390/w13050658.

Khan, M.Y.A., ElKashouty, M., Zaidi, F.K., Egbueri, J.C., 2023. Mapping aquifer recharge potential zones (ARPZ) using integrated geospatial and analytic hierarchy process (AHP) in an arid region of Saudi arabia. Rem. Sens. 15, 2567. https://doi.org/10.3390/rs15102567.

Kheradmand, S., Seidou, O., Konte, D., Batoure, M.B.B., 2018. Evaluation of adaptation options to flood risk in a probabilistic framework. J. Hydrol.: Reg. Stud. 19, 1–16. https://doi.org/10.1016/j.ejrh.2018.07.001.

Luo, Z., Fan, J., Shao, M., Hu, W., Yang, Q., Zhang, S., 2023. Soil water dynamics and groundwater evolutions of check dams under natural rainfall reduction in semi-arid areas. J. Hydrol. 617, 129099 https://doi.org/10.1016/j.jhydrol.2023.129099.

Majeed, M., Lu, L., Anwar, M.M., Tariq, A., Qin, S., El-Hefnawy, M.E., El-Sharnouby, M., Li, Q., Alasmari, A., 2023. Prediction of flash flood susceptibility using integrating analytic hierarchy process (AHP) and frequency ratio (FR) algorithms. Front. Environ. Sci. 10, 1037547 https://doi.org/10.3389/fenvs.2022.1037547.

Marjuanto, A.A., Putranto, T.T., Sugianto, D.N., 2019. Mapping of groundwater vulnerability index in the alluvial plain of Semarang city using the susceptibility index method. E3S Web of Conferences 125, 01010. https://doi.org/10.1051/e3sconf/201912501010.

Mondal, S., Maiti, R., 2013. Integrating the analytical hierarchy process (AHP) and the frequency ratio (FR) model in landslide susceptibility mapping of Shiv-Khola watershed, Darjeeling Himalaya. International Journal of Disaster Risk Science 4, 200–212. https://doi.org/10.1007/s13753-013-0021-y.

Moyo, C., Mishi, S., Ncwadi, R., 2022. Human capital development, poverty and income inequality in the Eastern Cape province. Development Studies Research 9 (1), 36–47.

Muavhi, N., Thamaga, K.H., Mutoti, M.I., 2022. Mapping groundwater potential zones using relative frequency ratio, analytic hierarchy process and their hybrid models: the case of Nzhelele-Makhado area in South Africa. Geocarto Int. 37, 6311–6330. https://doi.org/10.1080/10106049.2021.1936212.

Mukherjee, I., Singh, U.K., 2020. Delineation of groundwater potential zones in a drought-prone semi-arid region of east India using GIS and analytical hierarchical process techniques. Catena 194, 104681.

Oikonomidis, D., Dimogianni, S., Kazakis, N., Voudouris, K., 2015. A GIS/remote sensing-based methodology for groundwater potentiality assessment in Tirnavos area, Greece. J. Hydrol. 525, 197–208.

Opricovic, S., Tzeng, G.H., 2002. Multicriteria planning of post-earthquake sustainable reconstruction. Comput. Aided Civ. Infrastruct. Eng. 3, 211–220. https://doi.org/10.1111/1467-8667.00269.

Rafiei, F., Gharechelou, S., Golian, S., Johnson, B.A., 2022. Aquifer and land subsidence interaction assessment using sentinel-1 data and DInSAR technique. ISPRS Int. J. Geo-Inf. 11, 495. https://doi.org/10.3390/ijgi11090495.

Saaty, T.L., 1980. The Analytic Hierarchy Process: Planning, Priority Setting, Resource Allocation. McGraw, New York, NY, USA, p. 281.

Shekar, P.R., Mathew, A., 2023. Assessing groundwater potential zones and artificial recharge sites in the monsoon-fed Murredu river basin, India: an integrated approach using GIS, AHP, and Fuzzy-AHP. Groundwater for Sustainable Development 23, 100994. https://doi.org/10.1016/j.gsd.2023.100994.

Sherif, M., Sefelnasr, A., Al Rashed, M., Alshamsi, D., Zaidi, F.K., Alghafli, K., Baig, F., Al-Turbak, A., Alfaifi, H., Loni, O.A., 2023. A review of managed aquifer recharge potential in the Middle East and north Africa region with examples from the kingdom of Saudi arabia and the United Arab Emirates. Water 15, 742. https://doi.org/10.3390/w15040742.

Tariq, A., Beni, L.H., Ali, S., Adnan, S., Hatamleh, W.A., 2023. An effective geospatial-based flash flood susceptibility assessment with hydrogeomorphic responses on groundwater recharge. Groundwater for Sustainable Development 23, 100998. https://doi.org/10.1016/j.gsd.2023.100998.

Tweed, S.O., Leblanc, M., Webb, J.A., Lubczynski, M.W., 2007. Remote sensing and GIS for mapping groundwater recharge and discharge areas in salinity-prone catchments, in southeastern Australia. Hydrogeol. J. 15, 75–96.

Tzeng, G.H., Huang, J.J., 2011. Multiple Attribute Decision Making: Methods and Applications, vol. 1. CRC press, p. 352. https://doi.org/10.1201/b11032.

United Nations, 2015. Transforming Our World: the 2030 Agenda for Sustainable Development. United Nations, Department of Economic and Social Affairs, New York, NY. USA.

Urama, K.C., Ozor, N., 2010. Impacts of climate change on water resources in Africa: the role of adaptation. African Technology Policy Studies Network 29, 1–29.

Uvaraj, S., 2021. GIS based analytical hierarchy process (AHP) and frequency ratio (FR) models for groundwater potential zone mapping in Papanasam Taluk, Thanjavur district. International Journal of Geography, Geology and Environment 3 (2), 83–91.

van Breda Weaver, A., 1991. The distribution of soil erosion as a function of slope aspect and parent material in Ciskei, Southern Africa. Geojournal 23, 29–34.

Verdoodt, A., Van Ranst, E., Van Averbeke, W., 2003. Modelling crop production potentials for yield gap analysis under semiarid conditions in Guquka, South Africa. Soil Use Manag. 19 (4), 372–380.

Virupaksha, H.S., Lokesh, K.N., 2021. Electrical resistivity, remote sensing and geographic information system approach for mapping groundwater potential zones in coastal aquifers of Gurpur watershed. Geocarto Int. 36, 888–902. https://doi.org/10.1080/10106049.2019.1624986.

Woodford, A.C., Chevallier, L., 2002. Hydrogeology of the main Karoo basin: current knowledge and future research needs. Water Research Commission Report No. TT 179 (2), 482.

Yadav, B., Malav, L.C., Jangir, A., Kharia, S.K., Singh, S.V., Yeasin, M., Yadav, K.K., 2023. Application of analytical hierarchical process, multi-influencing factor, and geospatial techniques for groundwater potential zonation in a semi-arid region of western India. J. Contam. Hydrol. 253, 104122 https://doi.org/10.1016/j.jconhyd.2022.104122.

Zhao, X., Wang, D., Xu, H., Ding, Z., Shi, Y., Lu, Z., Cheng, Z., 2022. Groundwater pollution risk assessment based on groundwater vulnerability and pollution load on an isolated island. Chemosphere 289, 133–134. https://doi.org/10.1016/j.chemosphere.2021.133134.